JOURNAL OF THEORETICAL AND APPLIED MECHANICS
62, 3, pp. 547-560, Warsaw 2024
https://doi.org/10.15632/jtam-pl/188855

USE OF THE BIAXIAL COEFFICIENT IN DETERMINING LIFE FOR A COMBINATION OF CYCLIC BENDING AND TORSION OF BRONZE RG7

Joanna Małecka, Tadeusz Łagoda
Opole University of Technology, Opole, Poland
e-mail: j.malecka@po.edu.pl; t.lagoda@po.opole.pl

The paper proposes a new multiaxiality coefficient that can characterize fatigue tests for various combinations of bending and torsion. This coefficient can be defined depending on the criterion used. The factor is 1 for cyclic bending and 2 for pure torsion. Based on the fatigue tests of the RG7 bronze, analysis of calculation dispersion of the fatigue life was carried out concerning test results obtained through an experiment. This analysis was performed separately for individual tested combinations and for selected multiaxial fatigue criteria. The selected criteria are Huber-Mises, Gough-Pollard, maximum normal stress, maximum shear stress, and maximum normal and shear stress in the plane defined by shear stresses. The average values of the obtained durability were compared to the newly defined multiaxial coefficient distinguishing different combinations of bending and torsion. Fractographic analysis was also performed for selected samples for all four combinations of fatigue tests. It was found that the failure planes and design critical planes do not coincide.

Keywords: biaxial loading, life-time, bending and torsion, cyclic loading

More important nomenclatures

A_σ, m_σ – coefficients in fatigue characteristic for bending
A_τ, m_τ – coefficients in fatigue characteristics for torsion
cal, exp – calculated and experimental
E – elastic modulus
N_f – number of cycles to failure
r, r_{BF} – loading ratio and biaxial factor
$\Delta\tau$ – range of shear stresses
σ_a – amplitude of normal stress from bending
σ_u, σ_y – ultimate and yield stress
τ_a – amplitude of shear stress from torsion

1. Introduction

In the literature, we find numerous works on fatigue tests of cyclic bending with torsion of samples with a solid cross-section, i.e., in which stress and strain gradients for both bending and torsion are important. Less frequently, these are fatigue tests with cyclic tension-compression with torsion. In this case, thin-walled hollow samples are often used. In the case of torsion of thin-walled hollow samples, it does not give an additional effect of a stress gradient or strain. Then, the distribution of stresses and strains can be assumed to be homogeneous. These tests are described as cyclic bending or tension-compression $\tau_a = 0$, cyclic torsion $\sigma_a = 0$, and a combination of cyclic bending and torsion $\tau_a = k_{\tau/\sigma}\sigma_a$, where $k_{\tau/\sigma}$ is the ratio of shear to normal stresses. However, this does not describe the possible combinations uniformly. For this

purpose, a loading ratio has been proposed, which is defined in various ways. In the paper (Slamečka *et al.*, 2016), it was defined as

$$r = \frac{\sqrt{3}\tau_a}{\sigma_a + \sqrt{3}\tau_a} \tag{1.1}$$

But in the works (Slámečka *et al.*, 2010, 2013), it was defined as

$$r = \frac{\tau_a}{\sigma_a + \tau_a} \tag{1.2}$$

It can be seen that in the first case, the correction factor before the shear stress amplitude τ_a is $\sqrt{3}$, which is related to the Huber-Mises hypothesis, and in the second case, it is 1, which is related to the Galileo hypothesis. However, the defined loading ratio always ranges from 0 for cyclic bending (extension-compression) to 1 for cyclic torsion.

Another approach is also conceivable. Expressions can be written according to Tresca's hypothesis as

$$r = \frac{2\tau_a}{\sigma_a + 2\tau_a} \tag{1.3}$$

or the Gough-Pollard (Gough *et al.*, 1951) criterion, which is the most commonly used criterion for a proportional combination of cyclic bending and torsion in the form

$$r = \frac{1}{\sigma_a + \frac{\sigma_{a-1}}{\tau_{a-1}}\tau_a}\frac{\sigma_{a-1}}{\tau_{a-1}}\tau_q \tag{1.4}$$

However, we always get a result in the interval $(0, 1)$, and the final equation can be written as general equation

$$r_{LR} = \frac{k\tau_a}{\sigma_a + k\tau_a} \tag{1.5}$$

where k can be defined as $\sqrt{3}$ – Eq. (1.1), 1 – Eq. (1.2), 2 – Eq. (1.3), and σ_{a-1}/τ_{a-1} – Eq. (1.4) which is the fatigue strength ratio (Papuga *et al.*, 2021; Wächter *et al.*, 2022). If we are dealing with a brittle material, the value of this factor is 1.25, and if we are dealing with an extra ductile material, the value of this factor is > 1.75. However, it can be noticed that the proposed parameter has no physical significance, according to formulas (1.1)-(1.5), although it is very convenient to describe fatigue tests.

A slightly different approach can be found in (Susmel and Lazzarin, 2002) and later used, for example, in (Gan *et al.*, 2021), where a coefficient was introduced to modified fatigue characteristics, which, according to the authors, takes into account both multiaxiality and non-proportionality in the form

$$\rho = \frac{\sigma_{max}}{2\Delta\tau} \tag{1.6}$$

In this case, coefficient (1.6) becomes 0 for torsion and 1 for the axial load. This is opposite to coefficient r_{LR} (1.5). A completely different approach can be found in (Wang *et al.*, 2023) based on (Wang *et al.*, 2001). These papers propose a principal stress coefficient defined as

$$\gamma = \frac{\sigma_2 - \sigma_3}{\sigma_1 - \sigma_3} \tag{1.7}$$

The value of this coefficient determined on the basis of the principal stresses range from 0 to 1.

However, the fatigue life itself is determined using selected multiaxial fatigue criteria. Here, an appropriate criterion should (for example, presented in works (Kardas *et al.*, 2008; Karolczuk *et al.*, 2015; Carpinteri *et al.*, 2018; Łagoda and Macha, 1994; Niesłony *et al.*, 2014) be used to reduce a complex state of stress to an equivalent uniaxial one. Then, the fatigue life is determined based on the specified equivalent amplitude and fatigue characteristics for the uniaxial state of stress. Then, the computational durability is compared with the experimental one. Most often, both calculated and experimental lifetime are presented in a logarithmic system. The diagonal reflects perfect agreement of the calculation results with the experiment. The logarithmic system of axes corresponds to fatigue characteristics written as the logarithm of fatigue life. This approach can be found in many works. The first such an approach is most likely found in (Łagoda and Macha, 1994). It seems, however, that it would be possible to determine the average values of fatigue life dispersion for individual load combinations. Then, such a distribution can be compared with the dispersion for the uniaxial state of stress for particular combinations defined by Eq. (1.5) depending on the criterion used.

This work aims to propose such a biaxiality coefficient using the presented loading factor, which will be adequate to the selected applied criterion, taking into account the complex state of stress and especially various combinations of proportional bending and torsion. The verification of the proposal will be presented based on fatigue tests of bronze RG7 (Małecka and Łagoda, 2023a; Małecka *et al.*, 2023) performed by the authors of this paper. In addition, the work explains in detail the results, which may be used by other authors, of fatigue tests for this material, which have yet to be done before.

2. Biaxiality coefficient

The introduction presents proposals for different definitions of the loading ratio depending on a combination of bending and torsion. In the case of bending or tension-compression, we are dealing with a uniaxial state of stress. However, the matter could be more evident in the case of shear stresses. In this case, the shear stress can be applied by a torque for solid samples (Fig. 1a) or thin-walled hollow samples (Fig. 1b) to eliminate the stress and strain gradient effect. In both cases, we can talk about torsion about one axis. Shear stress can also be caused by technical shear, as shown in Fig. 1c. In this case, the axial force causes shear stress. Pure shear, on the other hand, is defined as simultaneous compression in one direction and tension in the other with the same force values as shown in Fig. 1d. Such fatigue tests have been presented, among others, on cross samples. The results of such tests for the 10HNAP material have been presented, among others, in work (Łagoda *et al.*, 2020). In this case, biaxial cyclic and random fatigue tests with a correlation coefficient of -1 result in pure shear fatigue. Therefore, switching from forces to stresses.

Figure 2a shows uniaxial fatigue tests, and Fig. 2c presents a pure shear stress state caused by a biaxial state of stress, where

$$\sigma_x = -\sigma_y \tag{2.1}$$

and in Fig. 2b, where we have an intermediate situation, i.e

$$\sigma_x = k_{x/y}\sigma_y \tag{2.2}$$

where $-1 < k_{x/y} < 0$. The loading factor known in the literature, presented in the general form by formula (1.5), apart from the fact that it distinguishes various combinations of normal and tangential loads with values from 0 to 1, has no other meaning. Since the uniaxial state is

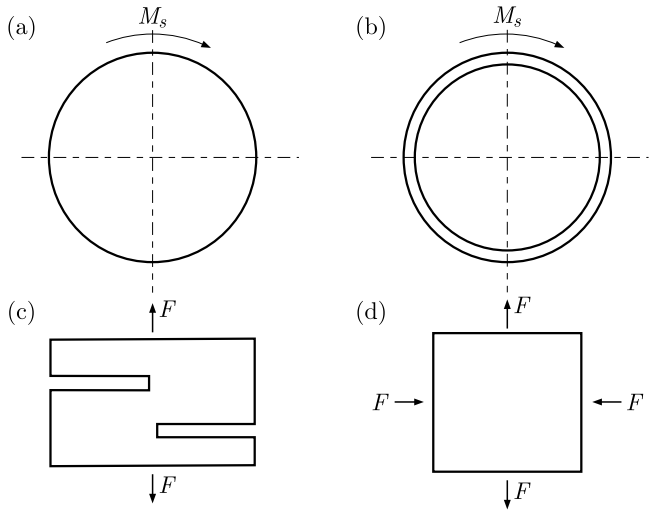

Fig. 1. Different ways to obtain shear stresses: (a) solid bar torsion, (b) tube torsion, (c) technical shear, (d) pure shear

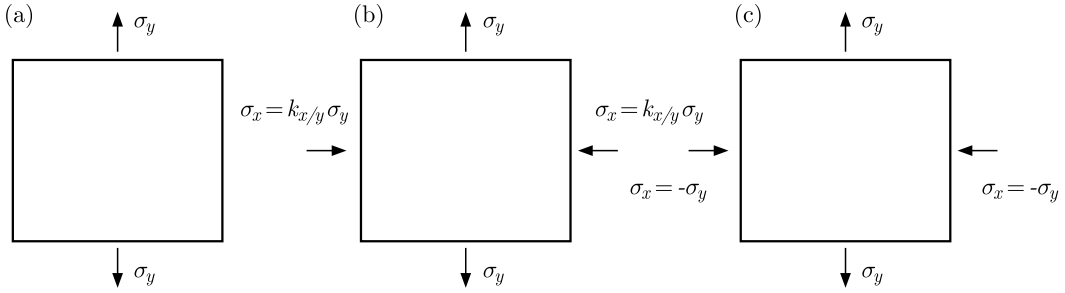

Fig. 2. Stress distribution for: (a) tension, (b) tension with shear, (c) pure shear

associated with the value 1, and the biaxial state with 2, it seems more logical to reformulate general formula (1.5) presented in this work with a new biaxial factor in the form

$$r_{BF} = 1 + \frac{k\tau_a}{\sigma_a + k\tau_a} \tag{2.3}$$

The value of this parameter r_{BF} reaches the minimum value for tension-compression (bending in the plane) equal to 1 (uniaxial load) and for maximum cyclic shear (two-sided torsion) equal to 2 (biaxial state). This means that pure bending reaches 1, and pure torsion values 2. However, the combination of bending and torsion is an intermediate value. The closer this value is to 2, it means that there is a more significant share of torsion. The k coefficient in Eq. (2.3) can be defined here depending on the criterion proposed by the researcher adopted for further calculations.

3. Experimental research and analysis

The fatigue tests concern the RG7 bronze alloy, also known as CuSn7Zn4Pb6. Its basic static properties are $E = 92.14\,\text{GPa}$, $\sigma_u = 270\,\text{MPa}$, $\sigma_y = 120\,\text{MPa}$. The basic chemical composition is Cu: 81%-86%, Sn: 5.2%-8%, Zn: 2%-5%, Pb: 5%-8% (Slamečka *et al.*, 2016; Susmel and Lazzarin, 2002). Tables 1-5 present the results of cyclical experiments in simple load conditions – tension-compression (Table 1), bending in a plane, and torsion on both sides (Table 2), and two combinations of proportional bending and torsion (Table 3). In the case of bending or torsion, nominal stress values are given, i.e., those that result from the given bending or torsion moment and the appropriate elastic section modulus for bending and torsion, respectively.

Table 1. Experimental results of RG7 copper alloy under axial tension-compression conditions

ε_a [‰]	σ_a [MPa]	N_{exp} [cycles]
3.0	192	5954
2.5	167	22556
2.2	162	73986
2.0	156	42000
1.8	136	137849
1.5	140	357851
1.3	–	> 2000000

Table 2. Experimental results of RG7 copper alloy in the conditions of in-plane cyclic

Bending		Torsion	
σ_{an} [MPa]	N_{exp} [cycles]	σ_{an} [MPa]	N_{exp} [cycles]
254	25850	163	17271
254	37723	158	35902
244	27766	158	3215
244	40511	153	171275
233	58327	153	93219
233	85021	143	19122
218	75647	143	70400
218	58069	143	86055
203	229748	135	289812
203	106173	135	785924
188	888016	127	650800
188	596720	127	481710
172	1592848	125	2499155
172	1135442	125	742896
152	1361954	117	3021316
152	571257	117	1349697
142	2011739	115	3215695
142	5827190	102	¿10000000
131	> 10000000		

Based on cyclical tests of the analyzed material, fatigue characteristics were determined according to the Basquin model, the double-logarithmic model, and the formulas according to (ASTM Standard 2003) – for in-plane bending and combinations of bending and torsion and two-sided torsion, respectively

$$\log N_f = A_\sigma - m_\sigma \log \sigma_a \qquad \log N_f = A_\tau - m_\tau \log \tau_a \tag{3.1}$$

The coefficients obtained according to equations (3.1) are summarized in Table 4.

The verification will be presented for several selected multiaxial fatigue criteria:

— Huber-Mises hypothesis

$$\sigma_{a\,eq} = \sqrt{\sigma_a^2 + 3\tau_a^2} \tag{3.2}$$

— Gough-Pollard hypothesis (Gough *et al.*, 1951)

$$\sigma_{a\,eq} = \sqrt{\sigma_a^2 + \left(\frac{\sigma_{a-1}}{\tau_{a-1}}\right)^2 \tau_a^2} \tag{3.3}$$

Table 3. Experimental results of RG7 copper alloy for the combination of cyclic bending and torsion

$\tau_{an} = 0.5\sigma_{an}$			$\tau_{an} = \sigma_{an}$		
σ_{an} [MPa]	τ_{an} [MPa]	N_{exp} [cycles]	σ_{an} [MPa]	τ_{an} [MPa]	N_{exp} [cycles]
177	88	42488	125	125	45085
177	88	59187	125	125	28808
166	83	89283	118	118	110665
166	83	88376	118	118	79988
144	72	136893	112	112	88149
144	72	136991	112	112	104546
133	67	776838	105	105	400352
133	67	424789	105	105	334607
122	61	919070	98	98	522700
122	61	1393731	98	98	896867
112	56	929541	91	91	435266
112	56	5691131	91	91	508131
102	51	> 5400000	84	84	> 10000000
101	50	5851778			
94	47	6058621			

Table 4. Coefficients according to the Basquin model according to formulas (3.1) for particular combinations of bending and torsion (Susmel and Lazzarin, 2002; Wächter *et al.*, 2022)

Bending		Torsion		$\tau_a = 0.5\sigma_a$		$\tau_a = \sigma_a$	
A_σ	m_σ	A_τ	m_τ	A_σ	m_σ	A_σ	m_σ
26.26	9.09	38.34	15.38	24.47	8.85	26.85	10.64

Hypothesis (3.2) and (3.3) have a similar formula, and in a particular case, when $\sigma_{a-1}/\tau_{a-1} = \sqrt{3}$, they are the same:
— maximum normal stress

$$\sigma_{a\,eq} = \sigma_{an,max} \tag{3.4}$$

— maximum shear stress

$$\sigma_{a\,eq} = 2\tau_{ans,max} \tag{3.5}$$

— maximum shear stress and normal stress in the critical plane defined by the maximum shear stress

$$\sigma_{a\,eq} = \Big(2 - \frac{\sigma_{a-1}}{\tau_{a-1}}\Big)\sigma_{an,max} + \frac{\sigma_{a-1}}{\tau_{a-1}}\tau_{ans,max} \tag{3.6}$$

Here, it should be noted that hypotheses (3.4)-(3.6), unlike (3.2) and (3.3), are linear criteria due to components of the stress state, and such criteria can also be dedicated to random or non-proportional loads (Mamiya *et al.*, 2011). Normal and shear stress for a combination of normal (from bending) and shear (from torsion) stresses at an angle α can be determined according to the formulas

$$\sigma_{an}(\alpha) = \cos(2\alpha)\sigma_a + \sin(2\alpha)\tau_a \qquad \tau_{ans}(\alpha) = -\frac{1}{2}\sin(2\alpha)\sigma_a + \cos(2\alpha)\tau_a \tag{3.7}$$

Critical planes for criteria (3.4)-(3.6) were determined for individual combinations of bending and torsion in accordance with formulas (3.7). The critical planes are defined by the angle α for

which the value of the amplitude, according to expressions (3.7), reaches its maximum value. The values of these angles are listed in Table 5, depending on the type of load. Table 5 also shows the positions of critical fatigue planes and experimental positions of the critical planes, which are presented in Figs. 3-6, and shows that the experimental failure planes coincide with the direction determined by the maximum normal stress.

Table 5. Setting the location of the critical planes and the macro-split plane of destruction [°]

	Bending	$\tau_a = 0.5\sigma_a$	$\tau_a = \sigma_a$	Torsion
$\sigma_{an,max}\alpha$	0	22.50	31.45	45
$\tau_{ans,max}\alpha$	45	67.50	76.45	90
Experiment	1.43	20.15	33.30	44.60

In connection with the proposed introduction of the biaxiality factor r_{BF}, it is possible to analyze how this coefficient translates into fracture fractography. Figures 3-6 shows photos of fracture surfaces for durability in the medium durability range, i.e. for durability of about 100 000 cycles. For in-plane bending (Fig. 3), i.e. with the biaxial fatigue factor $r_{BF} = 1$, the development of fatigue cracks can be seen from the two most distant points from the bending plane. In the case of two-sided torsion, i.e. when the biaxial fatigue factor reaches the value $r_{BF} = 2$, the fatigue crack (Fig. 4) may initiate on the entire external surface. In the intermediate case, i.e., a combination of bending and torsion, the proposed factor is within $(1, 2)$. Its exact value depends on the adopted methodology for determining this coefficient. In this case (Fig. 5), fatigue cracks begin to develop where the maximum normal stress occurs. The additional shear stress from torsion amplifies the fatigue cracking effect. A detailed analysis of fatigue cracks leads to the following conclusions. In the case of in-plane bending (Fig. 3), it is effortless to distinguish the fatigue zone and the residual zone, which are characteristic for fatigue fractures.

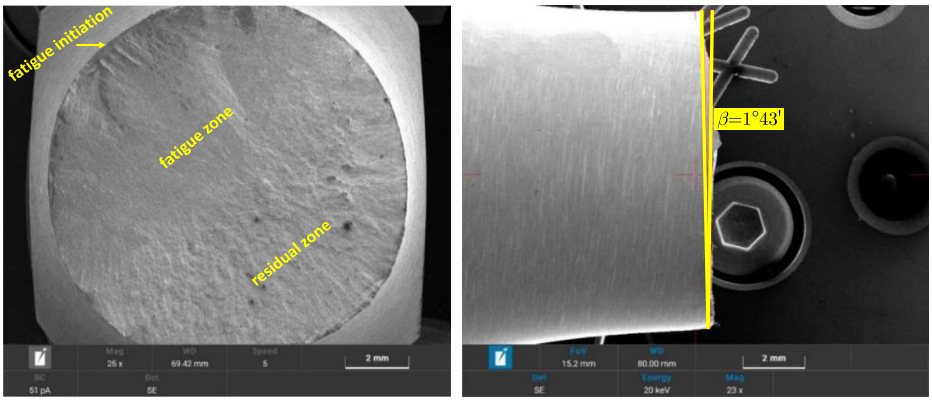

Fig. 3. Cyclic bending in a plane

However, a greater share of the fatigue zone concerning the residual zone is observed. At the fracture, a significant near-focal area is visible, along the edge of which a fatigue focus is visible in the form of characteristic fatigue lines, the distribution of which is not uniform. The surface of the fatigue zone at a low magnification seems smooth, which may indicate that the sample was subjected to a load with a low stress amplitude. In the case of cyclic torsion (Fig. 4), near--focus faults can be observed, which are already visible with the unaided eye. Parallel fatigue lines are observed in relation to the faults, and the morphology of the fracture surface indicates cleavage cracking along the grain sliding planes, as evidenced by the very finely developed surface topography. The branching of the faults, which a load change may have caused, is also clearly visible. For both bending and torsion combinations (Figs. 5-6), the fractures are characterized by a similar microrelief of the fatigue area topography throughout the area. Minor irregularities

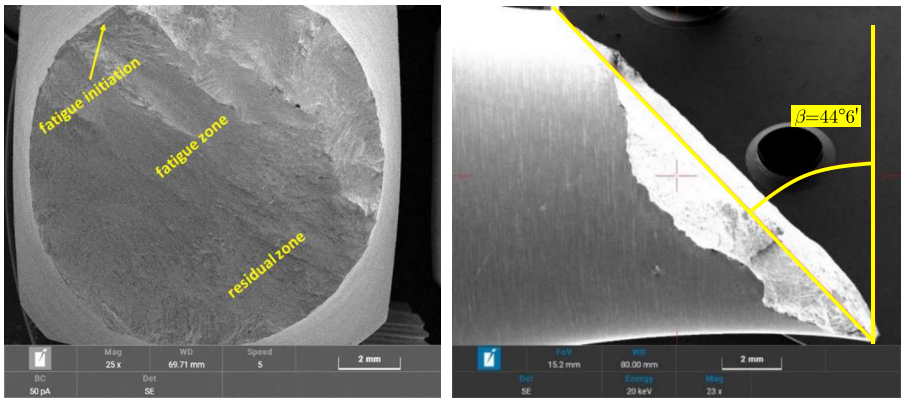

Fig. 4. Double-sided torsion

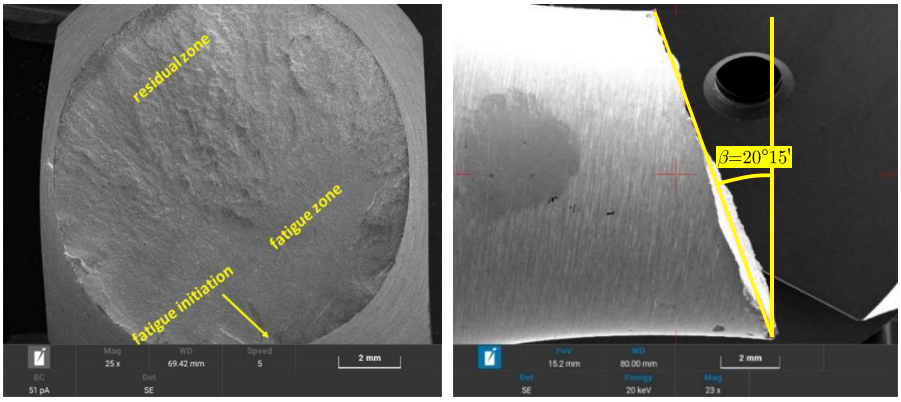

Fig. 5. Combination of cyclic bending with torsion $\tau_a = 0.5\sigma_a$

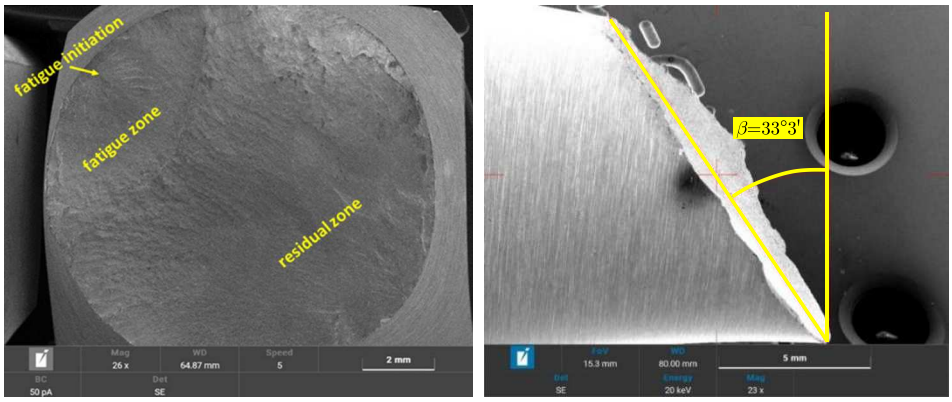

Fig. 6. Combination of cyclic bending with torsion $\tau_a = \sigma_a$

running deep into the fracture surface in the residual zone are noticeable. On the surface of both fractures, it is easy to locate the crack initiation site (fatigue focus visible in the fatigue zone), and it is also easy to identify mutually demarcating zones separating the fatigue zone band from the residual zone band. The surface of the residual zone is an area of a secondary scrap created by friction of the material during bending with torsion. The revealed properties of the scrap form the basis for considerations about the mechanism of initiation and development of fatigue cracks. From the analysis of the obtained images of fracture surfaces, it can be concluded that for each of the analyzed cases, the fatigue zone was formed in a long-term process of fatigue change growth as a result of crack propagation and spreading, and the residual zone was formed as a result of rapid destruction of the already weakened element.

4. Fatigue life according to multiaxial fatigue criteria

Table 6 lists the calculated multiaxial factors. These factors were derived depending on the multiaxiality criterion applied to the combination of proportional bending and torsion. The analysis of these coefficients shows that each time, in the case of cyclic bending, the multiaxiality factor is 1, and for cyclic torsion, it is 2. In the case of a combination of bending and torsion, this coefficient is between 1 and 2. In the case of criterion (3.6), the multiaxial coefficient can be defined in two ways. Both criteria (3.3) and (3.5) can be used here. A detailed analysis showed that for the combination of bending and torsion $\tau_a = 0.5\sigma + a$, this coefficient varies for the analyzed models within (1.33 and 1.50, and for the combination $\tau_a = \sigma_a$ within 1.50 and 1.63). Lower values are for criterion (3.5) – the criterion of maximum shear stresses, and greater for criterion (3.2) – Huber-Mises hypothesis.

Table 6. Multiaxial factors depending on the criterion and combination of bending and torsion

Criterion	Bending	$\tau_a = 0.5\sigma_a$	$\tau + a = \sigma_a$	Torsion
(3.2)	1	1.46	1.63	2
(3.3), (3.6)	1	1.43	1.60	2
(3.4)	1	1.33	1.50	2
(3.5), (3.6)	1	1.50	1.67	2

Then, analysis of the relationship between the obtained computational durability and those obtained as a result of the experiment was performed. Depending on the adopted criterion of multiaxial fatigue (3.2)-(3.6), the equivalent amplitude of normal stress was determined for all the obtained test results. This equivalent amplitude can be thought of as the stress amplitude from bending. Therefore, on the basis of fatigue characteristics $(3.1)_1$, the amplitude of cycles can be determined, where the design life is $N_{cal} - N_f$, based on the transformed characteristics in the form

$$N_{cal} = 10^{A_\sigma - m_\sigma \log \sigma_{aeq}} \tag{4.1}$$

For each of the analyzed characteristics, depending on the adopted criterion, the ratio of computational to experimental durability was determined for all experimental results. A linear approach can be found in the literature (Mamiya *et al.*, 2011) or a logarithmic one (Ma *et al.*, 2001)

$$d = \frac{N_{cal}}{N_{exp}} \qquad d = \log \frac{N_{exp}}{N_{cal}} \tag{4.2}$$

This paper used a linear relationship to analyze the dispersion given by formula (4.2). Then, the spreads mean values $\overline{d}$ and median d_m were determined. Table 7 shows the average values and median of fatigue life dispersion using selected multiaxial fatigue criteria (3.2)-(3.6). A scatter value of 1 means that the calculations perfectly agree with the experimental results. In the case of bending, the average error is close to 1. For the arithmetic mean value, it is slightly more (1.25), and for the median, it is less than 0.884. It follows that neither the mean nor the median value is a parameter that describes the mean value well in this case. Based on other studies, a parameter that would describe this phenomenon should be sought in the future. It may be a prime parameter combining these two average values. Coefficients close to 1 were obtained for torsion for criteria (3.3) and (3.6). This is because these criteria were derived from tests for cyclic bending and cyclic torsion.

For individual criteria, the results of calculating the mean values and the median are also presented in Figs. 7-12. In these figures, full points indicate average values. In these graphs, the

Table 7. Average/median life dispersion depending on the criterion used and the combination of bending and torsion

Criterion	Bending	$\tau_a = 0.5\sigma_a$	$\tau + a = \sigma_a$	Torsion
(3.2)	1.25/0.884	1.062/1.381	0.678/0.612	0.233/0.183
(3.3)	1.25/0.884	3.101/2.576	2.151/1.941	0.976/0.766
(3.4)	1.25/0.884	3.821/3.175	4.054/4.200	34.383/21.018
(3.5)	1.25/0.884	0.902/0.752	0.246/0.222	0.063/0.050
(3.6)	1.25/0.884	3.105/2.579	1.122/1.013	0.974/0.766

scatter band of 95% confidence, taking into account the 95% confidence interval for the mean value based on the standard error of the mean, is additionally marked by blank points. The horizontal line in each figure indicates compliance with the average value for cyclic bending. The analysis of the dispersion obtained in appropriate bands, depending on the criterion used and the multiaxiality coefficient, shows that none of the analyzed multiaxial fatigue criteria was consistent for all tested combinations of proportional cyclic bending with torsion in the 95% confidential interval band. It does not matter whether the arithmetic mean value or the median was taken as the mean value. In any case Gough-Pollard Criterion (3.3) and Maximum Normal Stresses (3.4) did not give satisfactory results. In the case of a small shear stress division, Huber-Mises criterion (3.2) and shear stress criterion (3.5) were effective. However, in the case of a large share of shear stresses, the criterion of shear and normal stresses determined by the maximum normal stress turned out to be effective (3.6). Therefore, it is proposed to use a hybrid criterion: shear stresses and shear and normal stresses determined by the maximum normal stress dependent on the multiaxiality factor in the form

$$\sigma_{aeq} = \begin{cases} 2\tau_{ans,max} & \text{for} \quad 1 \leqslant r_{BF} < \dfrac{3}{2} \\ \left(2 - \dfrac{\sigma_{a-1}}{\tau_{a-1}}\right)\sigma_{an,max} + \dfrac{\sigma_{a-1}}{\tau_{a-1}}\tau_{ans,max} & \text{for} \quad \dfrac{3}{2} \leqslant r_{BF} \leqslant 2 \end{cases} \tag{4.3}$$

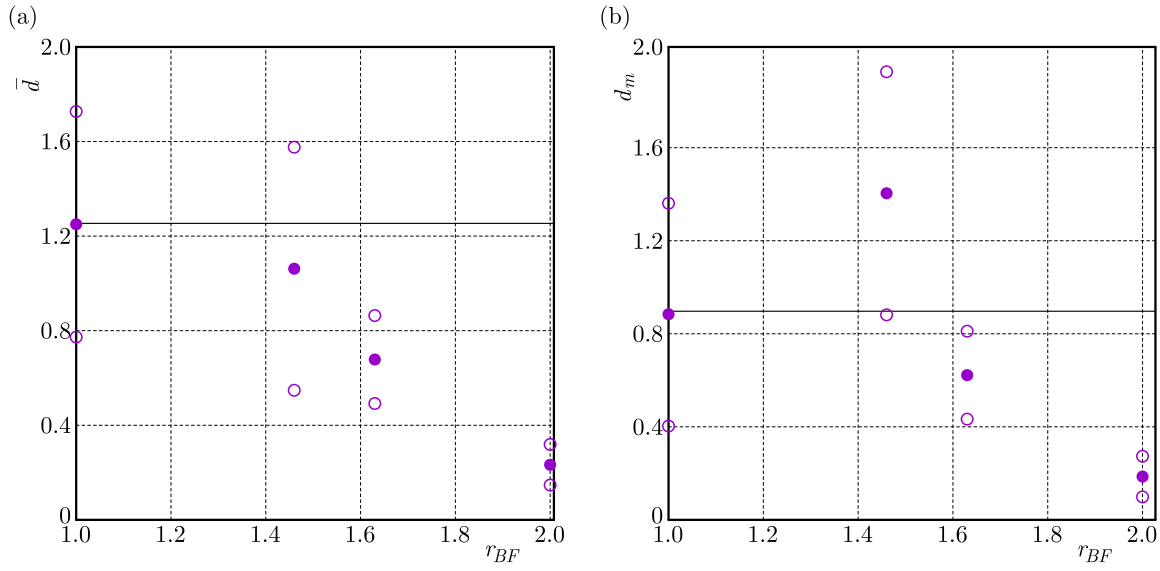

Fig. 7. Dispersion of the computational and experimental durability ratio for Huber-Mises criterion (3.2) with a probability coefficient of 95% depending on the multiaxiality factor: (a) mean value, (b) median value

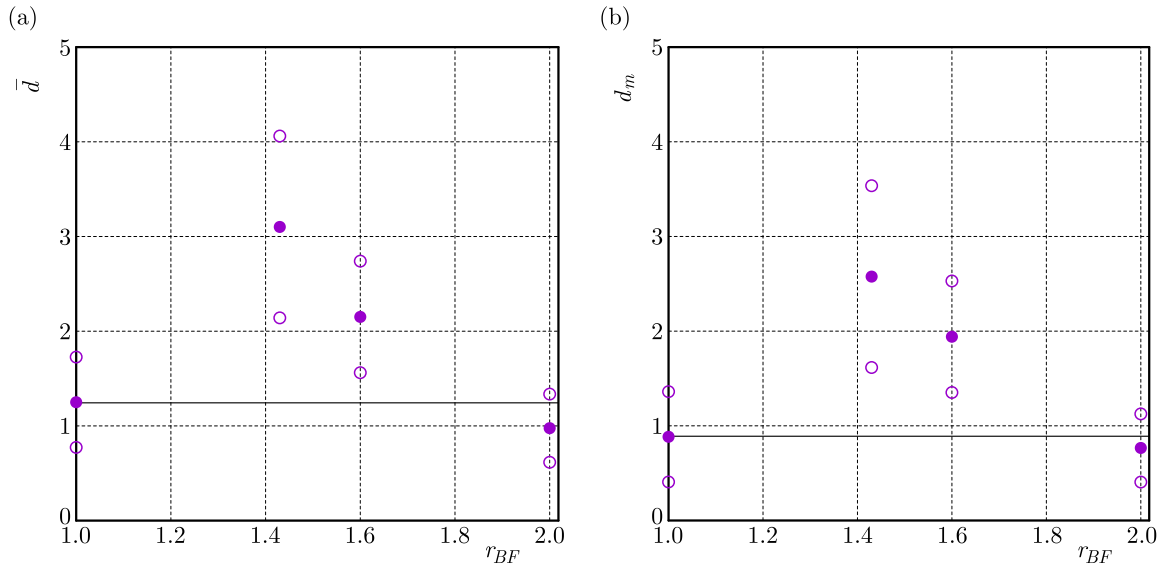

Fig. 8. Scatters of the computational and experimental durability ratio for Gough-Pollard criterion (3.3) with a probability coefficient of 95% depending on the multiaxiality factor: (a) mean value, (b) median value

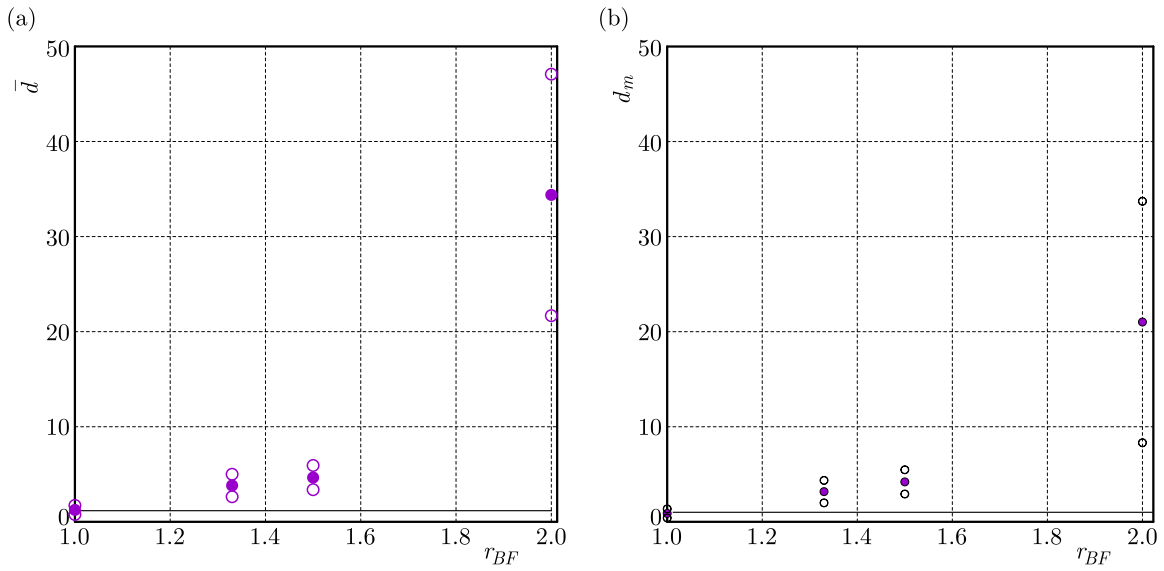

Fig. 9. Dispersion of the computational and experimental life ratio for criterion of maximum normal stresses (3.4) with a probability factor of 95% depending on the multiaxiality factor: (a) mean value, (b) median value

Analyzing the calculations in which critical planes were used, it turns out that the concepts of a critical plane and a crack plane are different. These concepts are not the same and mean completely other things. The values do not have to be the same either.

From the analysis of Table 7 and Figs, 7-12, it can be seen that in the case of mean values defined as average and median, the average value is always higher than that of the median value, except for one case. Additionally, it should be noted that the same situation applies to cyclic bending. Cyclic bending is the reference point in defining the multiaxial fatigue criterion. This value should be 1 for perfect compliance.

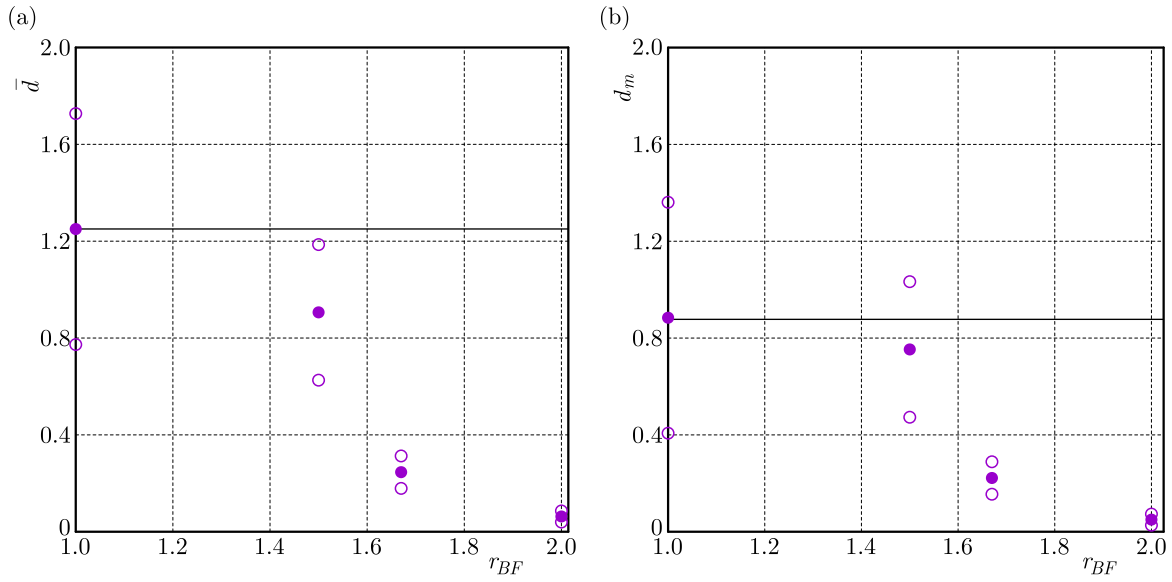

Fig. 10. Dispersion of the ratio of design and experimental life for criterion of maximum shear stresses (3.5) with a probability factor of 95% depending on the multiaxiality factor: (a) mean value, (b) median value

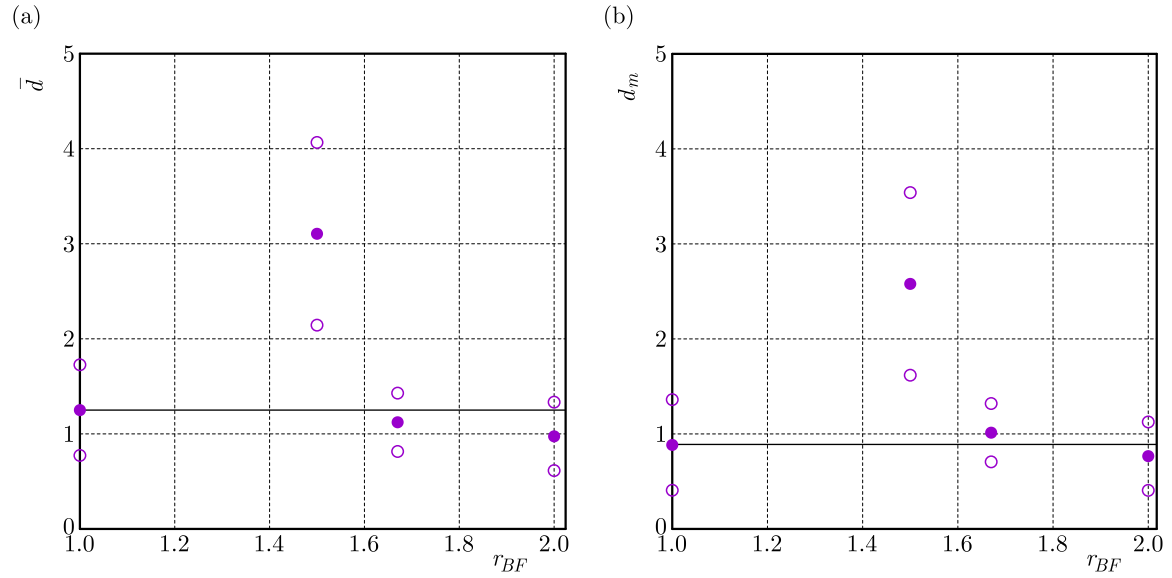

Fig. 11. Dispersion of the ratio of the design and experimental life for the criterion of maximum shear and normal stresses in the critical plane determined by maximum shear stresses (3.6) with a probability factor of 95% depending on the multiaxiality factor according to Tresca: (a) mean value, (b) median value

5. Conclusions

Based on the presented research results, the proposed models and presented analysis, it was found that:

- The new multiaxiality factor r_{BF} proposed in the paper, which can characterize fatigue tests for various combinations of bending and torsion, well characterizes multiaxiality.
- The proposed multiaxiality coefficient r_{BF} is a generalization of various coefficients found in the literature and can be selected depending on the criterion used.

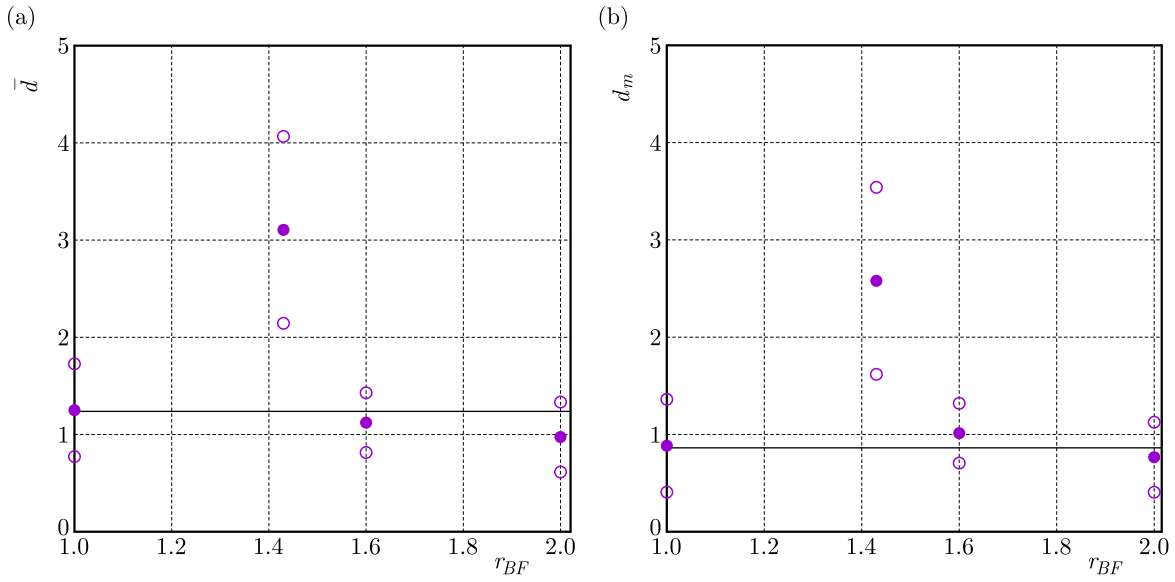

Fig. 12. Dispersion of the ratio of the design and experimental life for the criterion (maximum shear and normal stresses in the critical plane determined by maximum shear stresses (3.6) with a probability factor of 95% depending on the polyaxiality coefficient according to Gough-Pollard: (a) mean value, (b) median value

- The multiaxiality factor r_{BF} is 1 for cyclic bending and 2 for pure torsion. In the case of a combination of bending and torsion, the value of this factor is in the range $(1, 2)$.
- The analysis of the dispersion obtained in appropriate bands, depending on the criterion used and the multiaxiality factor, shows that none of the analyzed multiaxial fatigue criteria was consistent for all tested combinations of proportional cyclic bending with torsion in the 95% confidental interval band. It does not matter whether the arithmetic mean value or the median was taken as the mean value.
- In no case the Gough-Pollard criterion and the maximum normal stresses gave satisfactory results.
- In the case of a small branch of shear stresses, the Huber-Mises criterion and the shear stresses proved effective.
- In the case of a large share of shear stresses, the criterion of shear and normal stresses determined by the maximum normal stress turned out to be effective.
- It was proposed to use a hybrid criterion: shear and shear and normal stresses determined by the maximum normal stress dependent on the multiaxiality factor r_{BF}.
- The fractographic analysis of selected samples for all four combinations of fatigue tests showed that the occurrence of a fatigue center conditions the formation of the fatigue zone, the source of which is the concentration of stresses or an inhomogeneous structure of the material.
- The experimental failure planes are not coincident with the critical planes that are used first to determine the equivalent stresses and, consequently, the design life.

References

1. ASTM E1049-85, 2003, *Standard Practices for Cycle Counting in Fatigue Analysis*, The American Society for Testing and Materials, West Conshohocken, PA
2. Carpinteri A., Vantadori S., Łagoda T., Karolczuk A., Kurek M., Ronchei C., 2018, Fatigue assessment of metallic components under uniaxial and multiaxial variable amplitude loading, *Fatigue and Fracture Engineering Materials and Structures*, **41**, 1306-1317

3. Gan L., Wu, H., Zhong Z., 2021, Multiaxial fatigue life prediction based on simplified energy--based model, *International Journal of Fatigue*, **144**, 106036
4. Gough H.J., Pollard H.V., Clenshaw W.J., 1951, Some experiments on the resistance of metals to fatigue under combined stresses, *Aero Research Council*, **2522**, London: H.M.S.O
5. Kardas D., Kluger K., Łagoda T., Ogonowski P., 2008, Fatigue life of 2017 (A) aluminum alloy under proportional constant-amplitude bending with torsion in the energy approach, *Materials Science*, **44**, 541-549
6. Karolczuk A., Kurek M., Łagoda T., 2015, Fatigue life of aluminium alloy 6082 T6 under constant and variable amplitude bending with torsion, *Journal of Theoretical and Applied Mechanics*, **53**, 421-430
7. Łagoda T., Kurek M., Głowacka K., 2020, A formulation of the criterion for multiaxial fatigue in terms of complex number as proposed by Macha, *International Journal of Fatigue*, **133**, 105430
8. Łagoda T., Macha E., 1994, Estimated and experimental fatigue lives of 30CrNiMo8 steel under in- and out-of-phase combined bending and torsion with variable amplitudes, *Fatigue and Fracture Engineering Materials and Structures*, **17**, 1307-1318
9. Ma S., Markert B., Yuan H., 2001, Multiaxial fatigue life assessment of sitered porous iron under proportional and non-proportional loading, *International Journal of Fatigue*, **97**, 214-226
10. Małecka J., Łagoda T., 2023, Fatigue and fractures of RG7 bronze after cyclic torsion and bending, *International Journal of Fatigue*, **168**, 107475
11. Małecka J., Żak K., Łagoda T., 2023b, Fatigue fracture surface of bronze RG7 under proportional cyclic torsion and bending, *Measurement*, **218**, 113126
12. Mamiya E.N., Castro F.C., Algarte R.D., Araújo J.A., 2011, Multiaxial fatigue life estimation based on a piecewise ruled S-N surface, *International Journal of Fatigue*, **33**, 529-540
13. Niesłony A., Łagoda T., Walat K., Kurek M., 2014, Multiaxial fatigue behaviour of AA6068 and AA2017A aluminium alloys under in-phase bending with torsion loading condition, *Materialwissenschaft und Werkstofftechnik*, **45**, 947-952.
14. Papuga J., Margetin M., Chmelko V., 2021, Various parameters of the multiaxial variable amplitude loading and their effect on fatigue life and fatigue life computation, *Fatigue and Fracture Engineering Materials and Structures*, **44**, 2890-2912
15. Slamečka K., Pokluda J., Kianicová M., Horniková M., Major S., Dvorák I., 2010, Quantitative fractography of fish-eye crack formation under bending-torsion fatigue, *International Journal of Fatigue*, **32**, 921-928
16. Slamečka K., Pokluda J., Kianicová M., Horniková J., Obrtlik K., 2013, Fatigue life of cast Inconel 713LC with/without protective diffusion coating under bending, torsion and their combination, *Engineering Fracture Mechanics*, **110**, 459-467
17. Slámečka K., Šesták P., Vojtek T., Kianicová M., Hornková J., Šandera P., Pokluda J., 2016, A Fractographic study of bending/torsion fatigue failure in metallic materials with protective surface layers, *Advances in Materials Science and Engineering*, ID8952657
18. Susmel L, Lazzarin P., 2002, A bi-parametric Wohler curve for high cycle multiaxial fatigue assessment, *Fatigue and Fracture Engineering Materials and Structures*, **25**, 63-78
19. Wächter M., Linn A., Wuthenow R., Esderts A., Gaier Ch., Kraft J., Fllgren C., Vormwald M., 2022, On scaled normal stresses in multiaxial fatigue and their exemplary application to ductile cast iron, *Applied Mechanics*, **3**, 259-295
20. Wang Q., Lade P.V., 2001, Shear banding in true triaxial tests and its effect on failure in sand, *Journal of Engineering Mechanics*, **127**, 754-761
21. Wang Z., Pan P., Zuo J., Gao Y., 2023, A generalized nonlinear three-dimensional failure criterion based on fracture mechanics, *Journal of Rock Mechanics and Geotechnical Engineering*, **15**, 630-640

Manuscript received August 29, 2024; accepted for print January 29, 2024